Long-Term Reduction in Infrared Autofluorescence Caused by Infrared Light Below the Maximum Permissible Exposure

Benjamin D. Masella,[1,2] David R. Williams,[1–3] William S. Fischer,[3] Ethan A. Rossi,[2] and Jennifer J. Hunter[2,3]

[1]The Institute of Optics, University of Rochester, Rochester, New York, United States
[2]Center for Visual Science, University of Rochester, Rochester, New York, United States
[3]Flaum Eye Institute, University of Rochester, Rochester, New York, United States

Correspondence: Benjamin D. Masella, 55 Black Brook Road, Keene, NH 03431; bmasella@cvs.rochester.edu.

Submitted: June 7, 2013
Accepted: May 9, 2014

Citation: Masella BD, Williams DR, Fischer WS, Rossi EA, Hunter JJ. Long-term reduction in infrared autofluorescence caused by infrared light below the maximum permissible exposure. *Invest Ophthalmol Vis Sci*. 2014;55:3929–3938. DOI:10.1167/iovs.13-12562

Purpose. Many retinal imaging instruments use infrared wavelengths to reduce the risk of light damage. However, we have discovered that exposure to infrared illumination causes a long-lasting reduction in infrared autofluorescence (IRAF). We have characterized the dependence of this effect on radiant exposure and investigated its origin.

Methods. A scanning laser ophthalmoscope was used to obtain IRAF images from two macaques before and after exposure to 790-nm light (15-450 J/cm^2). Exposures were performed with either raster-scanning or uniform illumination. Infrared autofluorescence images also were obtained in two humans exposed to 790-nm light in a separate study. Humans were assessed with direct ophthalmoscopy, Goldmann visual fields, multifocal ERG, and photopic microperimetry to determine whether these measures revealed any effects in the exposed locations.

Results. A significant decrease in IRAF after exposure to infrared light was seen in both monkeys and humans. In monkeys, the magnitude of this reduction increased with retinal radiant exposure. Partial recovery was seen at 1 month, with full recovery within 21 months. Consistent with a photochemical origin, IRAF decreases caused by either raster-scanning or uniform illumination were not significantly different. We were unable to detect any effect of the light exposure with any measure other than IRAF imaging. We cannot exclude the possibility that changes could be detected with more sensitive tests or longer follow-up.

Conclusions. This long-lasting effect of infrared illumination in both humans and monkeys occurs at exposure levels four to five times below current safety limits. The photochemical basis for this phenomenon remains unknown.

Keywords: retina, light damage, radiation damage, scanning laser ophthalmoscopy, retinal pigment epithelium

Treatment and monitoring of retinal disease often require exposing the eye to illumination for imaging or surgery. Infrared (IR) illumination is often used because it is considered to be safer than visible light (<700 nm). Safety limits for long duration IR illumination are designed to prevent thermal and not photochemical damage.[1] Thus, acceptable IR exposure levels are often greater than those in the visible range, and commercial instruments often operate close to these limits. It has been previously shown that visible wavelengths lead to photochemical effects at exposure levels that had previously been thought to be below the damage threshold.[2–5] Here we seek to determine whether a similar effect occurs with exposure to IR light.

In 2008, Morgan et al.[3] reported that retinal radiant exposure to 568-nm light greater than or equal to 5 J/cm^2 causes a measurable decrease in the fluorescence of RPE lipofuscin excited at the same wavelength. They concluded that this visible autofluorescence (VAF) reduction is a photochemical effect, the extent of which is directly related to total retinal radiant exposure (RRE). They also tested the effect of 830-nm exposures on fluorescence excited at 568 nm. In this case, they found no significant VAF reduction.[2] In 2012, Hunter et al.[4] provided evidence that multiple fluorophores are involved in VAF reduction and, as a result, the action spectrum of this effect varies with the fluorescence excitation wavelength used to quantify it. Therefore, it is possible that infrared autofluorescence (IRAF), as described by Keilhauer and Delori in 2006,[6] may be susceptible to a similar form of reduction after exposure to IR wavelengths; however, this has not previously been observed.

Here we provide evidence that exposure to IR light causes a reduction in IRAF in monkeys and humans. In monkeys, we investigate the relationship between RRE and IRAF reduction. To understand whether this new finding is related to the light delivery method, we examined the relationship between the magnitude of this effect and the exposure method. We compared exposures using a custom-built adaptive optics scanning laser ophthalmoscope (AOSLO) and nonscanning, uniform-fields. Finally, we discuss the importance of IRAF reduction in the context of retinal light safety.

Table 1. Information Specific to Each Animal Studied

Animal	1	2
Species	*Macaca mulatta*	*Macaca fascicularis*
Sex	Female	Male
Age, y	14	19
Eye imaged	OD (right)	OD (right)
Axial length of imaged eye, mm	20.6 ± 0.10	19.0 ± 0.14
Corneal radius of curvature,* mm	6.35 ± 0.50	5.74 ± 0.07
Contact lens base radius of curvature, mm	6.25	5.95
Contact lens diameter, mm	10.0	12.2
Contact lens power, diopters	−3	−3

The table includes physiological information about the animal and the specific eye imaged as well as the parameters of the contact lens placed on that eye during all retinal imaging experiments.

* Radius of curvature reported is the mean of the measured vertical and horizontal radii.

Methods

Nonhuman Primates

All of the experiments in this study were performed using two macaque monkeys and were approved by the University of Rochester's Committee on Animal Resources; the study complied with the ARVO Statement for the Use of Animals in Ophthalmic and Vision Research. Specific information about the individual primates used is shown in Table 1. Before each imaging experiment, the animal was anesthetized for transport to the imaging laboratory with an injection of ketamine. Typically, 18 mg/kg was used; but, in some instances, as much as 21.5 mg/kg was necessary. When available, valium (0.25 mg/kg) also was used. Additionally, glycopyrrolate (0.017 mg/kg) and ketofen (5 mg/kg) were injected to reduce salivation and pain, respectively.

Approximately 30 minutes later, the animal was intubated and anesthetized with isoflurane gas. The isoflurane was mixed with pure oxygen, and its concentration was adjusted as necessary (typically between 1% and 4% isoflurane) to maintain the desired level of anesthesia. The rate of oxygen use ranged from 0.5 L per minute to 0.8 L per minute. During imaging, the animal was given lactated Ringer's solution via intravenous drip at a rate of 5 mL/kg per hour. Pupils were dilated and the eye cyclopleged with 1 to 2 drops each of phenylephrine hydrochloride (2.5%) and tropicamide (1%). A lid speculum was used to hold the imaged eye open and a hard contact lens protected the cornea and corrected the refractive error. A head post, gimbal mount, and three-axis stage were used to align the animal's head and pupil with the AOSLO and allow for stable control of retinal image location during IR exposures.

To prevent large eye movements, the animal was paralyzed with vecuronium bromide. This was delivered intravenously, first as a bolus (1 mg/kg) then continuously at a rate of 60 μg/kg per hour for the remainder of the experiment. While under anesthesia, the animal's vital signs were monitored continuously. The heart rate ranged from 130 beats per minute to 180 beats per minute, oxygen saturation was maintained at 100%, end-tidal CO_2 concentration ranged from 25% to 52%, and mean arterial pressure was always greater than 60 mm Hg.

To ensure the health of the animal, isoflurane anesthesia was limited to no longer than 6 hours for all experiments. Once the experiment was completed, the animal was given an additional 0.01 mg/kg of glycopyrrolate and 0.05 mg/kg of neostigmine to reverse the effect of the paralytic.

SLO Imaging

To image IRAF, a commercial confocal scanning laser ophthalmoscope (cSLO) (Spectralis HRA+OCT; Heidelberg Engineering, Heidelberg, Germany) was used to obtain 30-degree field-of-view images using each of the instrument's four imaging modalities: IR reflectance (815 nm), visible reflectance (red free, 488 nm), blue-light autofluorescence (excitation: 488 nm, emission: >510 nm), and IRAF (excitation: 785 nm, emission: 805–840 nm).

For all of the experiments in this study, changes in IRAF were measured by first obtaining cSLO images and then exposing the retina to IR illumination. Following IR exposures, the retina was imaged again with the cSLO. Cumulative RRE from all cSLO modalities was less than 0.2 J/cm^2. Pre- and postexposure cSLO images were compared to quantify any change in signal. To measure potential recovery of IRAF, follow-up imaging was performed 1 and 16 months after exposure.

IR Exposures

If IRAF reduction has a photochemical origin, the amount of reduction should depend on the cumulative flux delivered during the exposure. However, if the reduction has thermal origin, the amount of reduction should depend on the peak power delivered to the retina. To distinguish between these possibilities, we compared the IRAF reduction following two different methods of exposure: AOSLO scanned illumination and uniform illumination.

AOSLO, Scanned Illumination. Monkeys were imaged using an AOSLO designed specifically for primate imaging (Fig. 1). This has been described in detail previously.[7] It is a point-scanning system that sweeps a raster pattern on the retina at a frame rate of 25 Hz. Three illumination sources were used: an 850-nm laser diode (LD) for wavefront sensing, a 790-nm Δ17 nm superluminescent diode (SLD) for IR reflectance imaging, and a 680-nm Δ10 nm SLD for visible reflectance imaging. Wavefront sensing resulted in a cumulative exposure of less than 6% of the 790-nm RRE. To navigate the retina, reflectance imaging was performed using the 790-nm SLD on its lowest setting, which delivered 20 μW to the eye (cumulative exposure < 0.5 J/cm^2).

To test the effect of IR illumination on IRAF, retinal locations that had not been previously imaged using the AOSLO were illuminated with the 790-nm SLD. The scan field was rectangular, approximately 2 degrees per side. Each location received one of five retinal radiant exposures: 15, 22, 110, 220, or 450 J/cm^2. The parameters for these exposures are listed in Table 2. During each exposure, the retinal location was

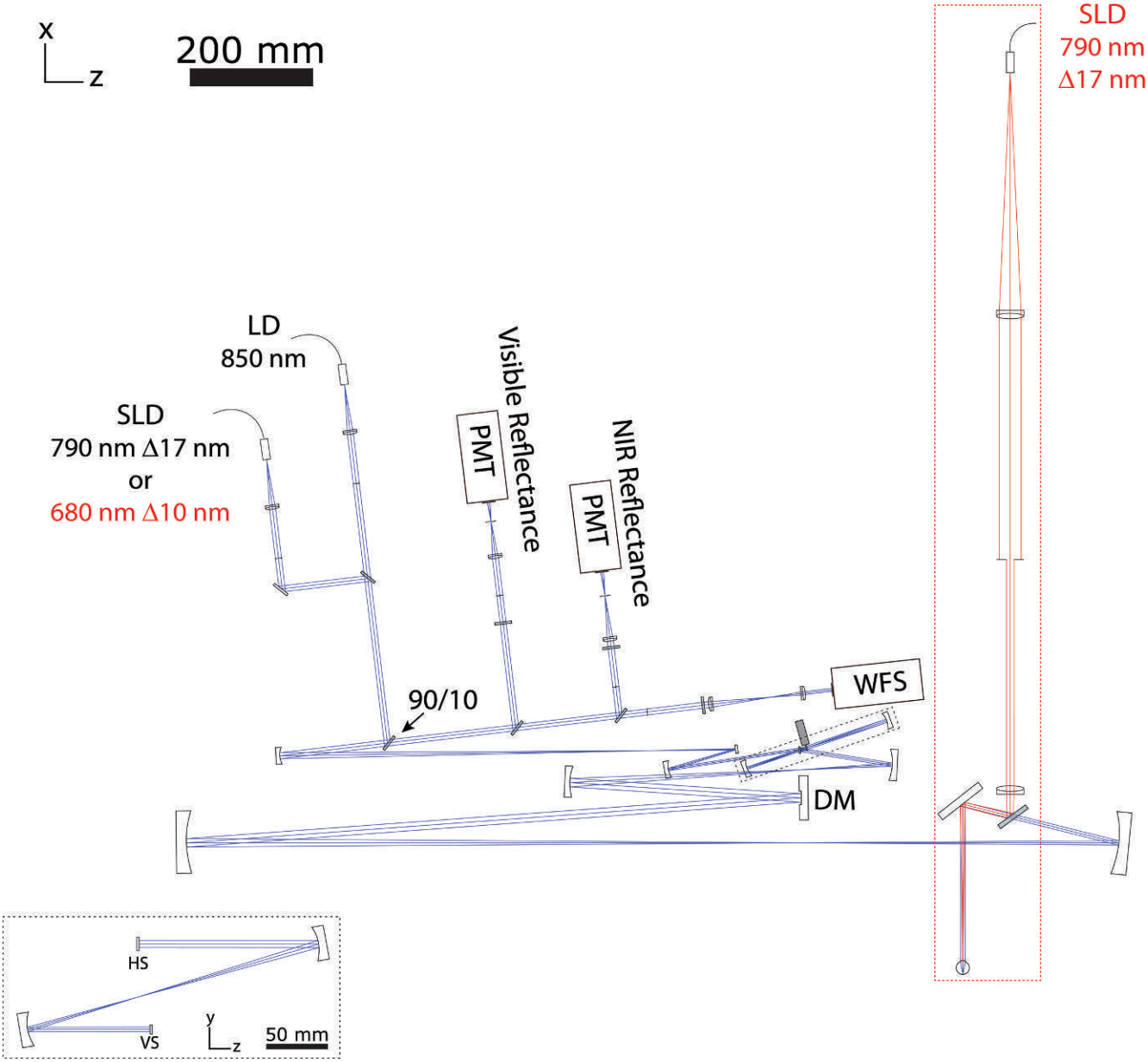

FIGURE 1. Optical layout of the adaptive optics scanning laser ophthalmoscope used in this study. Elements in the red dashed box represent the uniform illumination subsystem. Source wavelength data in *red* refers to the configuration during uniform illumination exposures.

carefully observed and small adjustments were made to correct for any eye drift. A short 790-nm reflectance video was recorded at the beginning of each exposure to document the retinal location. On rare occasions, the primate eye would drift farther than could be corrected. During these drifts, the exposure timer was paused and the SLD power reduced to its lowest setting until the eye returned to its original position and the exposure could be continued.

Uniform Illumination. A Maxwellian view illumination subsystem, similar to that used by Morgan et al.,[2] was integrated into the AOSLO. In a Maxwellian view configuration, the source is imaged to the entrance pupil of the eye, which limits the effect of the eye's aberrations on the incoming beam and allows a relatively large area of retina to be illuminated. The subsystem was designed to use the AOSLO's 790-nm SLD to illuminate a circular patch of retina with an area similar to the 2-degree raster scan. As shown in Figure 1, this subsystem was combined with the imaging path of the AOSLO using a pellicle beam-splitter (8% reflectance). To ensure uniform illumination, only the central portion of the Gaussian SLD beam (>95% of peak intensity) was used. The maximum power that could be delivered to the cornea was 25 μW. To match the 22 J/cm^2 AOSLO exposures, each retinal location was exposed for 18.5 minutes.

During exposures, the retina was imaged in reflectance using the 680-nm SLD to locate and maintain the exposure location. Cumulative exposure from the visible SLD was approximately 6 J/cm^2 in each tested location. The adaptive optics system was run in closed loop throughout; this had no impact on the uniform illumination channel. Reflected 790-nm illumination was imaged back through the IR channel of the AOSLO, allowing the position of the exposed region relative to the 680-nm image to be identified.

Table 2. Parameters for All IR Exposures

Delivery Method	RRE, J/cm^2	Power at the Cornea, μW	Duration, s	Repeated Trials, Animal 1	Repeated Trials, Animal 2	Repeated Trials, Human
AOSLO	15	325	126	6	0	0
AOSLO	22	330	183	6	0	0
AOSLO	110	340	900	8	2	0
AOSLO	~190*	300	~900	0	0	2
AOSLO	220	340	1800	2	2	0
AOSLO	450	340	3600	1	2	0
Uniform, centered	22	25	1110	3	0	0
Uniform, decentered	22	25	1110	3	0	0

With the exception of the 15 J/cm^2, 22 J/cm^2, and 450 J/cm^2 trials in animal 1, all AOSLO data were compiled from exposures performed during at least two imaging sessions. All uniform illumination data were obtained during a single imaging session. AOSLO and uniform illumination exposures were performed during imaging sessions approximately 2 weeks apart.

* Human AOSLO exposures were performed with a smaller field of view (1° × 1.85°) than those in the monkeys.

Uniform illumination experiments were designed to replicate, as closely as possible, all parameters of the AOSLO exposures except the spatial and temporal distribution of light on the retina. However, AOSLO and Maxwellian view systems produce very different spatial distributions of light at the pupil of the eye. With AOSLO exposures, each point within the exposed area is illuminated by a beam that is 7.2 mm in diameter at the pupil. With the uniform exposure, the entire retinal area is exposed to light that has passed through a focus at the center of the pupil. To test whether this difference in light distribution at the pupil has any impact on IRAF reduction, the output fiber tip of the SLD was mounted on a linear stage, which allowed it to be translated perpendicular to the optical axis. Because this source was conjugate to the entrance pupil of the eye, this translated the focus of the Maxwellian view system radially in the pupil. A second set of uniform exposures (RRE: 22 J/cm^2) was performed with the source focus decentered by 2.5 mm toward the bottom edge of the pupil.

Human Imaging

We also examined IRAF cSLO images from two human subjects who had participated in a separate AOSLO imaging study that delivered a cumulative RRE of approximately 150 J/cm^2 at 790 nm to one retinal location (~15° from the fovea) in one eye of each subject. This study was approved by the University of Rochester's Research Subjects Review Board and adhered to the tenets of the Declaration of Helsinki. During this separate study, these participants were imaged repeatedly in the same retinal location (field size was 1° horizontal and 1.85° vertical) for intervals of approximately 25 seconds, with a cumulative duration of 15 minutes over the course of 2.25 hours. Three wavelengths were used: 850 nm, 790 nm, and 488 nm. Cumulative RREs at each wavelength were approximately 13.0 ± 2.5 J/cm^2, 190 ± 40 J/cm^2, and 0.25 ± 0.04 J/cm^2, respectively. IRAF images were obtained 1 day after exposure using the cSLO described above as well as with a Spectralis HRA, which used the same excitation wavelength (785 nm) but collected a larger emission bandwidth (> 805 nm). Additional IRAF images were taken weekly using the Spectralis HRA+OCT for 4 weeks following the exposures.

Between 1 and 6 days after AOSLO imaging, each subject was evaluated with a comprehensive eye examination to determine whether any retinal changes could be observed clinically in the exposed retinal areas. An ophthalmologist performed direct ophthalmoscopy of the retina, carefully focusing on the exposed retinal area and retinal areas adjacent to the exposure location. Visual function was assessed clinically with visual acuity testing and Goldmann visual fields. To determine any possible change in visual function at the exposure locations, participants also underwent testing with multifocal electroretinography (mfERG, Veris Science 5.0; Electro-Diagnostic Imaging, Inc., Redwood City, CA, USA) and microperimetry (Centervue; MAIA, Padova, Italy). Microperimetry testing was performed using the standard macular assessment test, as well as using a customized test pattern that tiled the exposed retinal area and adjacent locations. To test for any statistically significant difference in sensitivity, the microperimetry test spots inside and outside the exposed area were compared using a Student's *t*-test.

Data Processing

To quantify IRAF changes, each cSLO image was manually aligned by overlaying, centering, and rotating them using Adobe Photoshop (Adobe Systems, Inc., San Jose, CA, USA). For the AOSLO exposures, the center of each exposed area was located using 790-nm reflectance images recorded with the AOSLO. Next, the mean intensity measured within a square region (500 × 500 μm; 110 × 110 pixels) centered on the exposed area was calculated and divided by the mean intensity of two 500 × 250-μm regions adjacent to the nasal and temporal sides of the exposure (see Fig. 2). Finally, the ratio was divided by that measured in the same location before the IR exposures. This IRAF ratio is a metric analogous to the visible AF ratio used by Morgan et al.[3] An IRAF ratio less than 1 corresponds to a decrease in IRAF. To characterize the variability of this measurement, IRAF ratios were calculated for regions within the cSLO images that had not been exposed to IR light in the AOSLO.

For uniform illumination exposures, the center of each exposed area was located by comparing the 680-nm and 790-nm reflectance images recorded with the AOSLO to the aligned cSLO images. As the Maxwellian view system illuminates a circular region of retina, the mean intensity was measured within the largest square region of pixels contained within the exposed area. The IRAF ratio was then calculated in the same manner as for the AOSLO exposures.

Statistical Analysis

To test the effect of RRE on the IRAF ratio, an ANOVA was performed. In addition, the IRAF ratio for each RRE was compared to the control data using a two-tailed Student's *t*-test, assuming equal variance. This same test was used to identify significant differences between exposure paradigms. For longitudinal analysis, paired *t*-tests were used. No correction for multiple comparisons was applied in any of the analyses. A *P* value less than 0.05 was deemed significant.

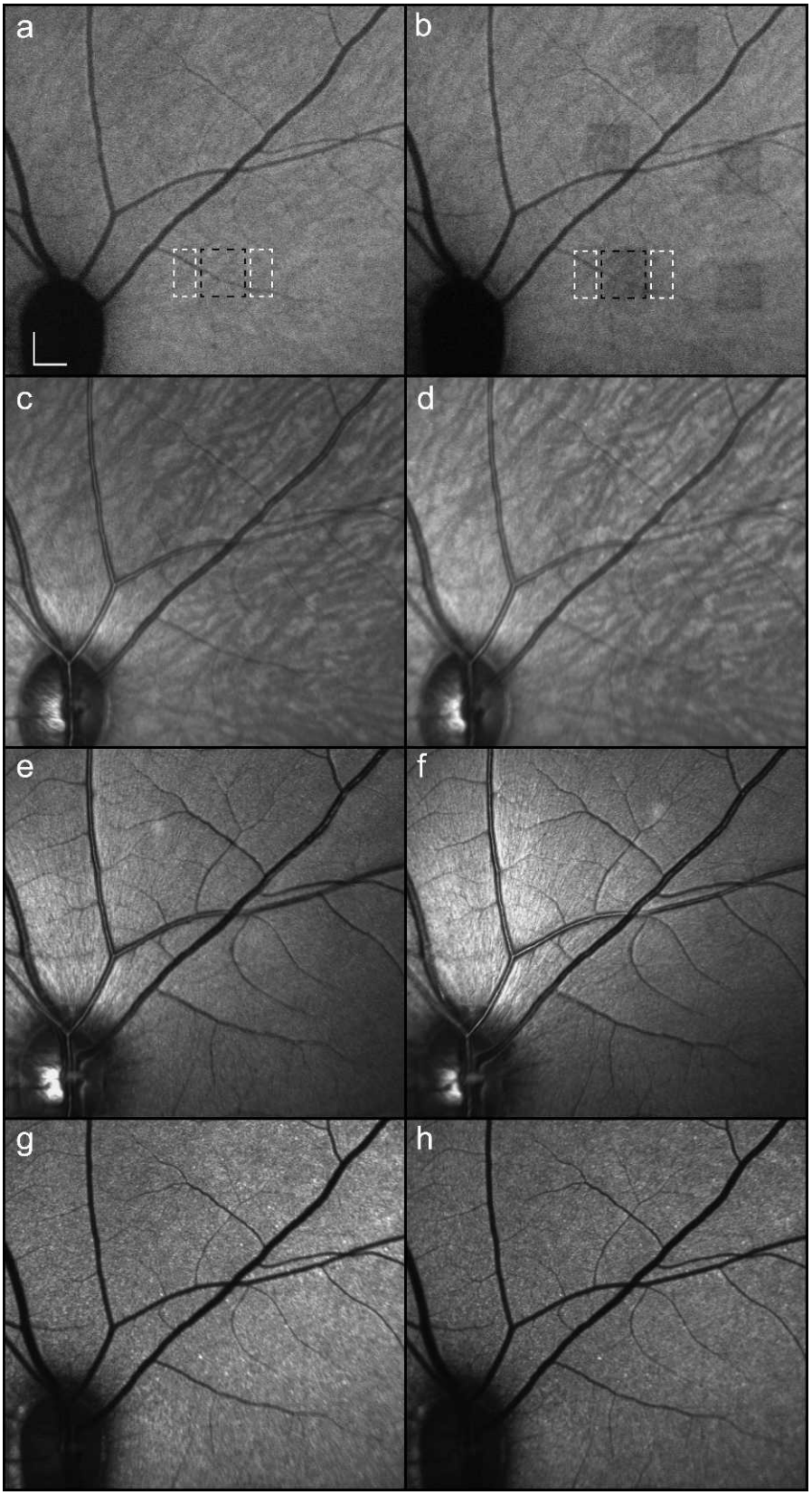

FIGURE 2. Example IRAF (**a**, **b**), IR reflectance (**c**, **d**), red-free (**e**, **f**), and VAF (**g**, **h**) images of animal 1 less than 3 hours before (**a**, **c**, **e**, **g**) and less than 3 hours after (**b**, **d**, **f**, **h**) five 110 J/cm^2, 790-nm exposures in the AOSLO. *Dashed boxes* denote example areas used for measurement (*black*) and normalization (*white*) of IRAF signal within an exposed region. *Scale bar*: 400 μm.

Investigative Ophthalmology & Visual Science

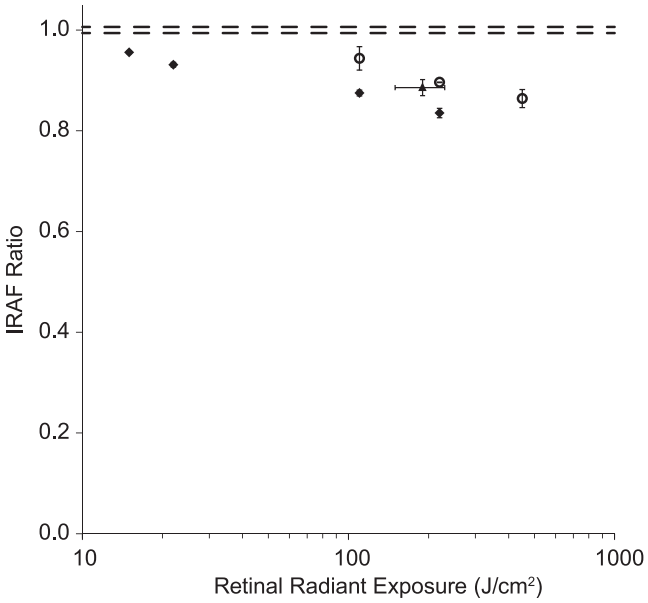

FIGURE 3. Measured IRAF reduction for all AOSLO exposures tested. The *diamonds* and *open circles* represent data from two different animals. The *triangular data point* is the mean IRAF reduction measured in the two human subjects. *Error bars* are 1 SE from the mean. The *dashed lines* represent 1 SE from the mean of three control measurements.

RESULTS

Effect of Radiant Exposure in Monkeys

All retinal exposures tested caused a significant decrease in IRAF ratio ($P < 0.001$). Figure 2 shows representative images of retinal areas exposed to 110 J/cm^2, taken using each cSLO modality. The lowest retinal radiant exposure tested, 15 J/cm^2, caused a 4% mean reduction in IRAF. Given the SD of the AOSLO measurements, the smallest difference that could be reliably measured with this method is approximately 1%. The magnitude of IRAF reduction increased with RRE (Fig. 3). As shown in Figure 4, no significant decrease in signal was measured in the IR reflectance, blue-light AF, or red-free modes of the Spectralis ($P = 0.13$, 0.66, and 0.39, respectively). Although the delay between each RRE and its respective IRAF measurement varied from 10 minutes to more than 3 hours, no significant variation was found in the magnitude of initial IRAF reduction for a given RRE ($P = 0.60$).

Tracking IRAF reduction over time showed slow recovery. One month after exposure, IRAF signal was measured in locations exposed to 110, 220, and 450 J/cm^2. The IRAF ratio in these locations remained significantly reduced compared with control areas ($P = 0.010$, $P < 0.001$, and $P < 0.002$, respectively). No significant recovery was measured for the 110 J/cm^2 exposures after 1 month. However, as is shown in Figure 5, at the same time point, partial recovery of IRAF ratio was measurable for the 220 and 450 J/cm^2 exposure levels ($P = 0.020$ and $P < 0.007$, respectively). Images in these locations taken 21 months after IR exposure showed no significant IRAF reduction when compared with control measurements ($P = 0.850$, 0.170, and 0.204, respectively, see Fig. 5).

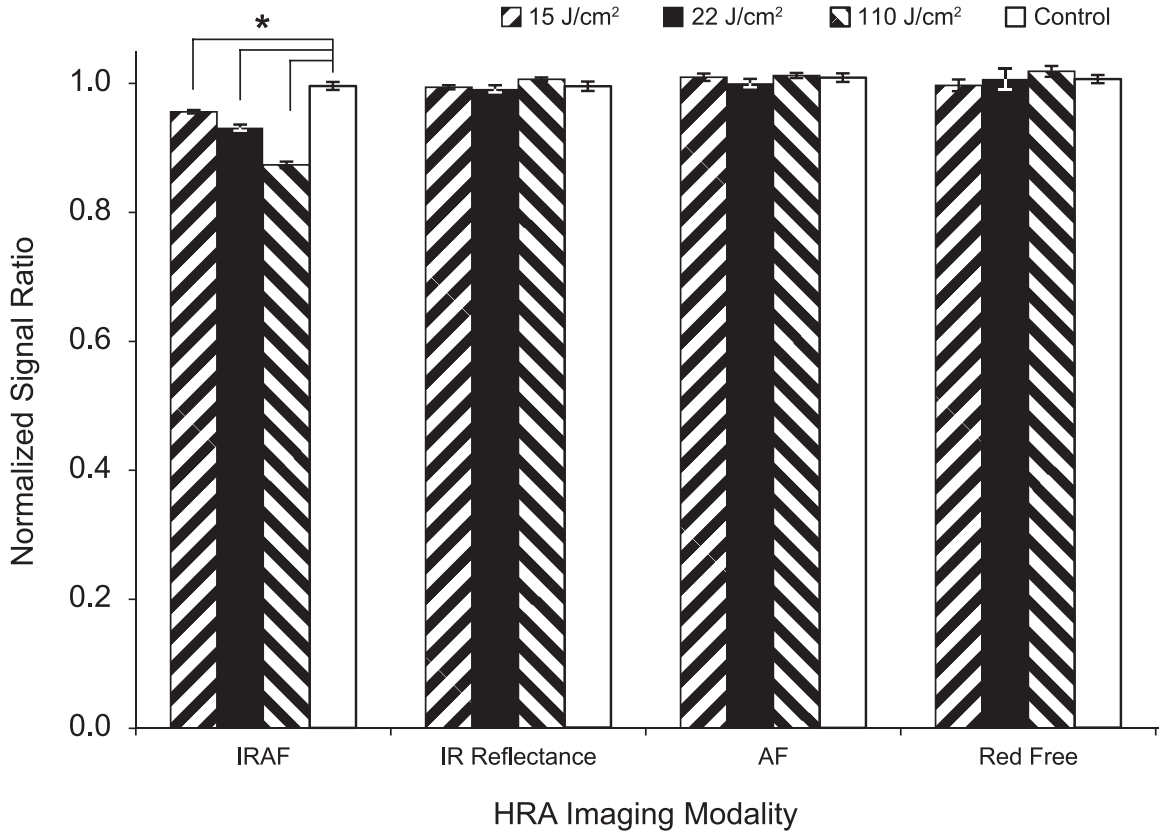

FIGURE 4. Normalized signal ratios from all Spectralis modalities following 790-nm exposures compared with modality-specific control measurements. All data shown are from animal 1. The *error bars* represent 1 SE from the mean.

Investigative Ophthalmology & Visual Science

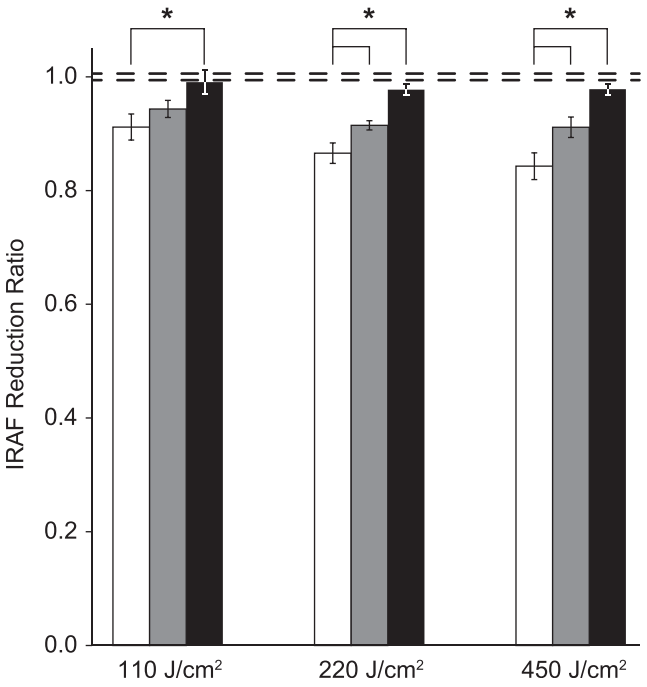

FIGURE 5. A comparison of IRAF ratios measured immediately (*white bars*, *left*), 1 month (*gray bars*, *middle*), and 21 months (*black bars*, *right*) after exposure. The 220 J/cm² and 450 J/cm² RREs showed significant recovery of IRAF signal after 1 month ($P = 0.020$ and < 0.007, respectively). All RREs tested showed recovery after 21 months. IRAF ratios at 21 months were not significantly different from control measurements at any RRE ($P = 0.850$, 0.170, and 0.204, respectively). Mean data from both animals are shown. *Error bars* show the SEM. The *dashed lines* represent 1 SE from the mean of three control measurements.

Uniform Illumination and Pupil Centration Experiments

As shown in Figure 6, no significant difference was measured between AOSLO and uniform illumination exposures ($P = 0.16$). Additionally, no significant difference in IRAF reduction was found between uniform illumination focused at the center of the pupil and uniform illumination with a decentered focus ($P = 0.85$). Because of the directional sensitivity of the retina,[8] the comparison of the effects of uniform and scanned retinal exposures must also consider a possible influence of the difference in the distribution of light passing through the pupil. The scanned field on the retina was formed from light with a uniform intensity distribution filling a 7.2-mm pupil, whereas the uniform exposure on the retina was formed from light focused to a tiny point, approximately 60 μm in diameter at the pupil. If the Stiles-Crawford effect had an impact on the magnitude of IRAF reduction, one would expect that the Maxwellian view configuration of the uniform exposure would result in a larger reduction for a given average RRE. The expected drop in cone coupling efficiency for a 2.5-mm displacement would be approximately 40%[9,10] but one would expect this to be mitigated by the fact that the cones account for only approximately 16% of the retinal area in the exposed regions and the fact that the rods have substantially broader directional tuning. As seen in Figure 6, no difference in IRAF reduction between the centered and decentered illumination was measured. This suggests that if the waveguiding effects of photoreceptors have an influence on IRAF reduction at all, it is not large enough to complicate the comparison of uniform and scanned retinal exposures.

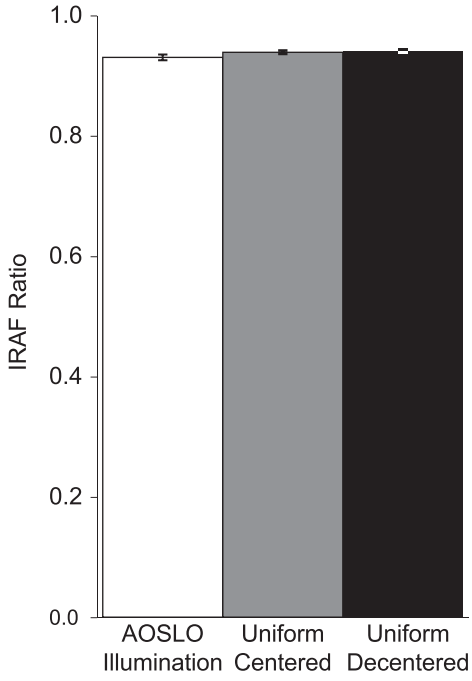

FIGURE 6. IRAF ratios measured after AOSLO illumination (*white bar*, *left*) or uniform illumination with different pupil centering (centered or decentered down by 2.5 mm). No significant difference was found between AOSLO and uniform illumination ($P = 0.16$), or between centered (*gray bar*, *middle*) and decentered (*black bar*, *right*) uniform illumination ($P = 0.85$).

Human Results

Infrared autofluorescence reduction was observed in both human subjects after RREs of approximately 190 J/cm². Figure 7 shows the effect of IR exposure in both human subjects. The magnitude of reduction (an average reduction of 12% between the two subjects) was consistent with that observed for similar exposures in monkeys. Over the course of the subsequent 4

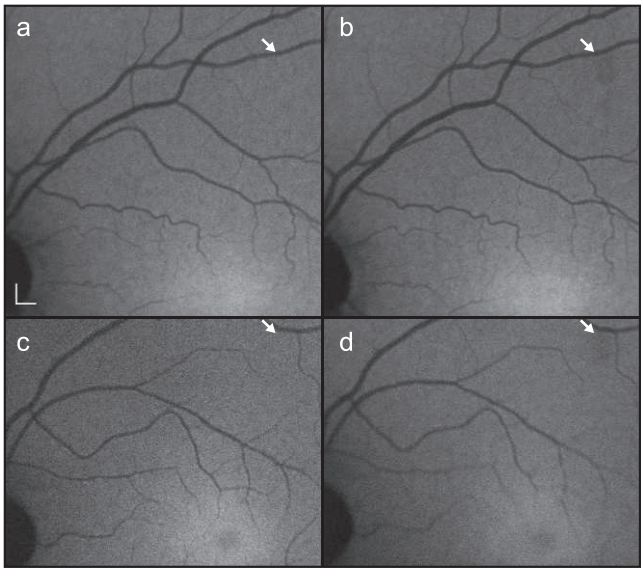

FIGURE 7. Example IRAF images from two human subjects before (**a**, **c**) and after (**b**, **d**) cumulative 790-nm exposures of approximately 190 J/cm² in the AOSLO. *White arrows* denote the exposure locations. *Scale bar*: 400 μm.

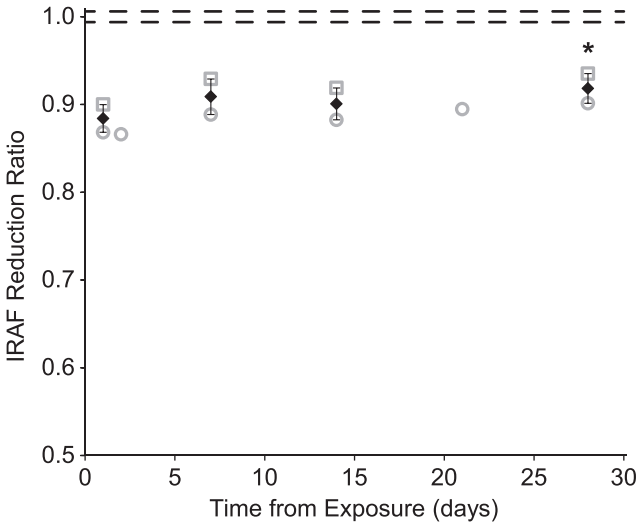

FIGURE 8. IRAF reduction measurements as a function of time from RRE in two human subjects. Individual subject measurements are shown as *open squares* and *open circles*. *Black diamonds* represent the mean of the two subjects. *Error bars* are the SEM. Recovery of IRAF signal is slow but statistically significant within 28 days ($P = 0.021$). The *asterisk* denotes significant difference from the 1 day post measurement.

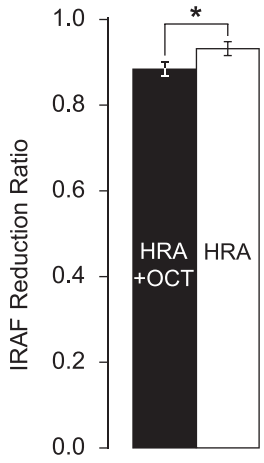

FIGURE 9. Comparison of IRAF reduction in human subjects measured with the Spectralis HRA+OCT and Spectralis HRA. Paired *t*-test shows significantly different measurements ($P = 0.004$). *Error bars* are 1 SE from the mean.

weeks, there was a small but significant recovery of IRAF signal, consistent with the primate result ($P = 0.021$, Fig. 8). As can be seen in Figure 9, IRAF reduction measurements made within 1 day of IR exposure with the Spectralis HRA, which collects a broader emission bandwidth than the Spectralis HRA+OCT, showed a significantly reduced effect ($P = 0.004$). Figure 10 shows the threshold photopic sensitivity measurements from each participant. The mean threshold attenuation measured outside the area of IR exposure was 28.4 ± 0.60 dB, whereas that measured inside was 29.5 ± 0.35 dB. These values were not significantly different ($P = 0.27$). Visual acuity, Goldmann visual fields, and mfERG were normal for both participants.

DISCUSSION

Properties of IRAF Reduction

Infrared autofluorescence reduction is almost certainly a photochemical rather than a thermal effect. The IR exposures performed in this study should have caused less than a 0.5°C increase in local temperature.[11] Thermal damage to the retina typically occurs when retinal temperature is increased by at least 10°C,[12] 20 times greater than the thermal increase we estimate we produced. For an individual cell within the exposed region, the raster scan of the AOSLO produces several intense pulses of IR energy at the line scan rate (~15 kHz) repeated at the system frame rate (25 Hz). In contrast, in the uniform illumination scheme, each cell is illuminated continuously with a lower irradiance. Although the scanned exposures produce larger peak changes in temperature than uniform illumination, no difference in IRAF reduction was observed, which also argues against a thermal origin. On the other hand, the similarity in IRAF reduction despite the large difference in the spatio-temporal pattern of light delivery shows that it is the total exposure that is key in determining the amount of reduction observed, as expected if the phenomenon has a photochemical origin.[4]

Infrared autofluorescence reduction is greater when measured with an instrument with a narrower spectral bandwidth for light collection. We observed this by comparing the IRAF reduction with the Spectralis HRA+OCT and the Spectralis HRA, the former collecting light from 805 to 840 nm and the latter collecting all fluorescence beyond 805 nm. This difference implies that the source of the IRAF signal comprises the combined emission of multiple fluorophores, only a subset of which is selectively bleached by the 790-nm illumination. A prediction of photobleaching is that it should be visible immediately after light exposure. We have not yet confirmed this prediction because the minimum time between exposure and measurement in our experiments was 10 minutes.

Relation to Visible Autofluorescence Reduction

Infrared autofluorescence reduction is similar to previously reported VAF reduction[3] in that both appear to have a photochemical origin. Moreover, both appear rapidly after exposure to illumination at wavelengths close to the excitation peak of the fluorescence of interest. This supports the view that the excitation spectrum for autofluorescence is actually the envelope of the excitation spectra of a rather large number of bleachable molecular species, each with their own peak wavelength and relatively narrow excitation spectrum. These effects differ, however, in their rate of recovery and magnitude of response to RRE. Visible autofluorescence reduction has been shown to recover within hours after the initial exposure.[4] Infrared autofluorescence signal shows very slow recovery (see Figs. 5, 8) and remains significantly reduced relative to the preexposed condition for months after exposure.

In vitro studies of VAF reduction in cultured RPE cells laden with the bisretinoid A2E, a major component of RPE lipofuscin, were performed by Yamamoto et al.[13] Using mass spectrometry, they found evidence suggesting that photooxidation is the primary factor in VAF reduction. The possibility of such a photoreaction leading to the formation of reactive oxygen species that could harm the RPE is a concern when considering a potential cumulative effect of these exposures. It is unknown whether IRAF reduction also represents a photooxidation of the fluorophores involved or a less harmful photoisomerization.

Unlike VAF, whose source, lipofuscin, is normally confined to the RPE, the fluorescence measured in a standard IRAF

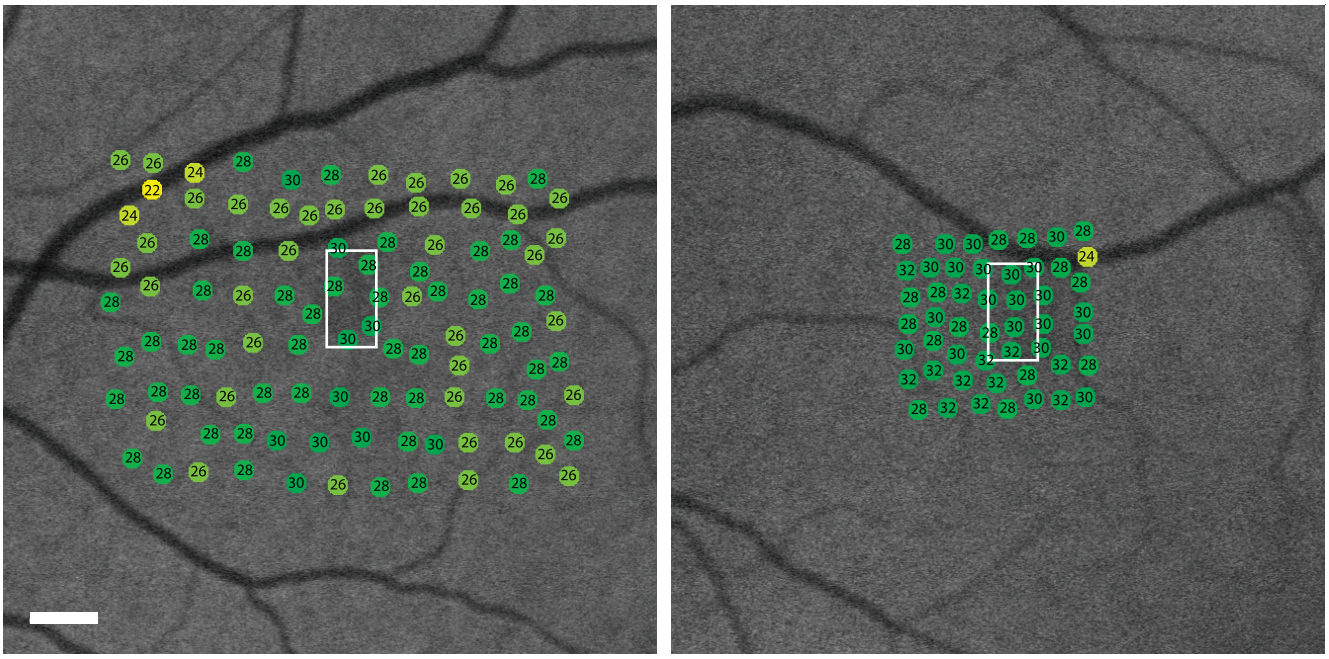

Figure 10. IRAF images showing the retinal locations in which photopic sensitivity was tested in the two human subjects using the Centervue MAIA microperimeter. The values shown represent the measured threshold attenuation in decibels. The *white boxes* denote the location of IR exposure. No significant difference in threshold attenuation was found between areas tested inside and outside the exposed regions ($P = 0.27$). *Scale bar*: 400 μm.

instrument is thought to arise from melanin in both the RPE and choroid.[6] Measurements in older human subjects suggest that as much as 50% to 60% of the IRAF signal is choroidal in origin.[6] Although this ratio is likely affected by the denser pigmentation of nonhuman primates, as well as the smaller emission bandwidth of the current measurements, reduced signal from either the retina or choroid could contribute to the measured reduction. Each monkey tested in this study appears to have very different susceptibilities to IRAF reduction (Fig. 3). The current cohort of two animals is not enough to determine whether variables such as relative pigmentation or absolute IRAF signal are related to this susceptibility.

As shown in Figure 4, no significant change in any other cSLO imaging modality, including IR reflectance and blue-light AF, was measurable. If retinal melanin is affected by these IR exposures, the effect does not measurably deplete or shift its absorption in the visible or IR. This again suggests that these exposures are affecting a secondary fluorophore that contributes to IRAF. However, there are currently too few data to support such a claim, and more work is needed to determine whether this reduction constitutes a chemical change that could be cumulatively harmful to the retina.

Comparison of Exposures to Current Safety Limits

The American National Standards Institute (ANSI) defines its maximum permissible exposure (MPE) to protect against potential thermal, photochemical, and mechanical damage to the retina. With the relatively low light intensities used in this study, mechanical damage was not a concern. Also, the current ANSI standard considers photochemical effects only in the visible regime and no photochemical limit is defined above 600 nm. As a result, ophthalmic instruments often capitalize on IR illumination wavelengths to operate at higher RREs.

The exposures investigated in this study fall into a range governed solely by the thermal MPE, which is directly proportional to the fourth root of exposure duration. Because of this, the varied durations used to produce each RRE for these experiments require that each time and power combination be compared to a different MPE value. The MPE for each RRE tested was calculated by applying the rules for calculating the ANSI MPE for an SLO as described by Morgan et al.[2] All AOSLO exposures were below the MPE for this AOSLO at 790

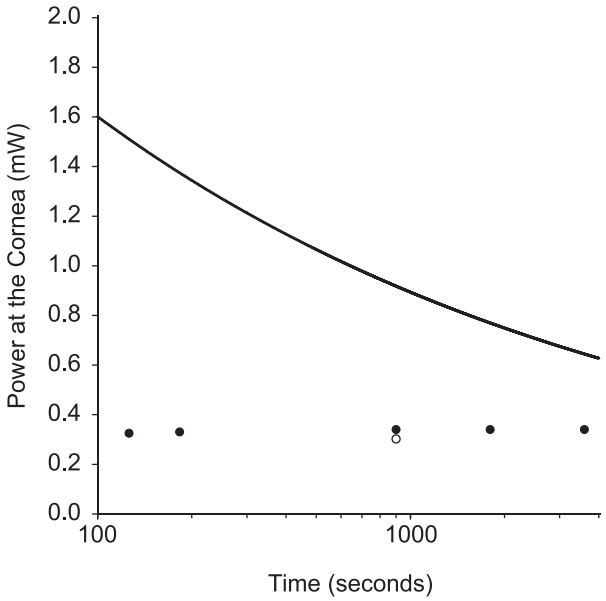

Figure 11. Maximum permissible exposure (MPE) of 790 nm shown in milliwatts at the cornea as a function of exposure duration calculated for our monkey AOSLO exposure parameters (*solid line*). The AOSLO exposures tested in this study (monkey: *filled circles*, human: *open circle*) are all below the MPE.

nm (Fig. 11). Retinal radiant exposures tested ranged from 22% to 53% of the MPE (ANSI Z136.1).[1]

Photopic microperimetry was the most sensitive and regionally specific functional test performed on the two human subjects. There was no significant difference in sensitivity in the area where IRAF reduction was observed. However, the slow recovery rate of IRAF is concerning. It may be necessary to revisit the potential for photochemical interactions due to IR exposure. Until any possible long-term or cumulative effects of this phenomenon are better understood, it is unclear whether it will be necessary to further limit retinal IR exposure, taking this long recovery time into account. We did not attempt to define an exposure threshold below which IRAF does not occur. Because of the apparent photochemical nature of this effect, it is likely that any threshold we measure would be indicative only of the minimum sensitivity of our measurement to changes in IRAF signal.

Conclusions

Exposure to IR illumination causes a reduction in IRAF at light levels as low as four to five times below the current MPE defined by the ANSI. The extent of this IRAF reduction is not affected by the distribution of light at the pupil or the retina. It appears to be solely a function of RRE, which suggests a photochemical process. No other sign of retinal change has yet been observed following IR exposure. Further study is needed to determine whether IRAF reduction should be a factor in determining the maximum permissible IR exposure for ophthalmic instruments.

Acknowledgments

The authors thank Lee Anne Schery and Mina M. Chung, MD, for their assistance.

Supported by the National Institutes of Health, Bethesda, Maryland (Grants BRP-EY014375, R01-EY022371, R01-EY004367, K23-EY016700, P30-EY001319, and T32-EY07125). The image registration software used to produce our AOSLO images, DeMotion, was developed by Alfredo Dubra and Zach Harvey with funding from Research to Prevent Blindness and the National Institutes of Health through Grants BRP-EY014375 and 5 K23 EY016700. Alfredo Dubra and Kamran Ahmad developed the adaptive optics control software.

Disclosure: **B.D. Masella**, None; **D.R. Williams**, Bausch and Lomb (F), Polgenix (F), Canon, Inc. (F), Welch Allyn (F), Pfizer (C), P; **W.S. Fischer**, None; **E.A. Rossi**, None; **J.J. Hunter**, Polgenix (F)

References

1. ANSI. American National Standard for Safe Use of Lasers ANSI Z136.1-2007. Orlando, FL: Laser Institute of America; 2007.
2. Morgan JI, Hunter JJ, Masella B, et al. Light-induced retinal changes observed with high-resolution autofluorescence imaging of the retinal pigment epithelium. *Invest Ophthalmol Vis Sci*. 2008;49:3715–3729.
3. Morgan JI, Hunter JJ, Merigan WH, Williams DR. The reduction of retinal autofluorescence caused by light exposure. *Invest Ophthalmol Vis Sci*. 2009;50:6015–6022.
4. Hunter JJ, Morgan JI, Merigan WH, Sliney DH, Sparrow JR, Williams DR. The susceptibility of the retina to photochemical damage from visible light. *Prog Retin Eye Res*. 2012;31:28–42.
5. van Norren D, Gorgels TG. The action spectrum of photochemical damage to the retina: a review of monochromatic threshold data. *Photochem Photobiol*. 2011;87:747–753.
6. Keilhauer CN, Delori FC. Near-infrared autofluorescence imaging of the fundus: visualization of ocular melanin. *Invest Ophthalmol Vis Sci*. 2006;47:3556–3564.
7. Hunter JJ, Masella B, Dubra A, et al. Images of photoreceptors in living primate eyes using adaptive optics two-photon ophthalmoscopy. *Biomed Opt Express*. 2010;2:139–148.
8. Stiles WA, Crawford BH. The luminous efficiency of rays entering the eye pupil at different points. *Proc R Soc Lond B Biol Sci*. 1933;112:428–450.
9. Moon P, Spencer DE. On the Stiles-Crawford effect. *J Opt Soc Am*. 1944;34:319–329.
10. Applegate RA, Lakshminarayanan V. Parametric representation of Stiles-Crawford functions: normal variation of peak location and directionality. *J Opt Soc Am A*. 1993;10:1611–1623.
11. Mainster MA, White TJ, Tips JH, Wilson PW. Retinal-temperature increases produced by intense light sources. *J Opt Soc Am*. 1970;60:264–270.
12. Clarke AM, Geeraets WJ, Ham WT Jr. An equilibrium thermal model for retinal injury from optical sources. *Appl Opt*. 1969; 8:1051–1054.
13. Yamamoto K, Zhou J, Hunter JJ, Williams DR, Sparrow JR. Toward an understanding of bisretinoid autofluorescence bleaching and recovery. *Invest Ophthalmol Vis Sci*. 2012;53: 3536–3544.

Investigative Ophthalmology & Visual Science